NIH Public Access
Author Manuscript
J Mol Cell Cardiol. Author manuscript; available in PMC 2011 January 1.

Published in final edited form as:
J Mol Cell Cardiol. 2010 January ; 48(1): 172. doi:10.1016/j.yjmcc.2009.07.028.

Age-Dependent Changes in Na Current Magnitude and TTX-Sensitivity in the Canine Sinoatrial Node

Lev Protas[1], **Ronit V. Oren**[3], **Colleen E. Clancy**[3,4], and **Richard B. Robinson**[1,2]

[1]Department of Pharmacology, College of Physicians and Surgeons, Columbia University, New York, NY

[2]Center for Molecular Therapeutics, College of Physicians and Surgeons, Columbia University, New York, NY

[3]Department of Physiology and Biophysics, Institute for Computational Biomedicine, Weill Medical College of Cornell University, New York, NY

Abstract

In rabbit, sodium current (I_{Na}) contributes to newborn sinoatrial node (SAN) automaticity but is absent in adult SAN, where heart rate is slower. In contrast, heart rate is high and I_{Na} is functional in adult mouse SAN. Given the slower heart rates of large mammals, we asked if I_{Na} is functionally active in SAN of newborn or adult canine heart. SAN cells were isolated from newborn (6–10 days), young (40–43 days) and adult mongrels. I_{Na} was observed in >80% of cells from each age. However, current density was markedly greater in newborn, decreasing with age. At all ages, I_{Na} was sensitive to nanomolar tetrodotoxin (TTX); 100 nmol/L inhibited I_{Na} by 46.7%, 59.9% and 90.7% in newborn, young and adult cells, respectively. While high TTX sensitivity suggested the presence of non-cardiac isofoms, steady-state inactivation was relatively negative (midpoints −89.7±0.7 mV, −95.1±1.2 mV and −93.4±1.9 mV from newborn to adult). Consequently, I_{Na} should be unavailable at physiological potentials under normal conditions, and 100 nmol/L TTX did not change cycle length or action potential parameters of spontaneous adult SAN cells. However, computer modeling predicts the large newborn I_{Na} protects against excess rate slowing from strong vagal stimulation. The results show that canine SAN cells have TTX–sensitive I_{Na} which decreases with post-natal age. The current does not contribute to normal automaticity in isolated adult cells but can be recruited to sustain excitability if nodal cells are hyperpolarized. This is particularly relevant in newborn, where I_{Na} is large and parasympathetic/sympathetic balance favors vagal tone.

Keywords

sinoatrial node; pacemaker; Na current; development; computer simulation

© Published by Elsevier Ltd.

Corresponding Author: Lev Protas, M.D/Ph.D., Columbia University, Department of Pharmacology, 630 West 168 Street, PH7West-318, New York, NY, 10032, Phone: 212-305-1573, Fax: 212-305-8780, lp141@columbia.edu .
[4]Current address: Department of Pharmacology, University of CA Davis, Davis, CA Running title: Na current in canine sinoatrial node

Publisher's Disclaimer: This is a PDF file of an unedited manuscript that has been accepted for publication. As a service to our customers we are providing this early version of the manuscript. The manuscript will undergo copyediting, typesetting, and review of the resulting proof before it is published in its final citable form. Please note that during the production process errors may be discovered which could affect the content, and all legal disclaimers that apply to the journal pertain.

DISCLOSURES
None

NIH-PA Author Manuscript
NIH-PA Author Manuscript
NIH-PA Author Manuscript

NIH-PA Author Manuscript

NIH-PA Author Manuscript

NIH-PA Author Manuscript

INTRODUCTION

The mammalian heartbeat is initiated in the sinoatrial node (SAN), where proper automatic function requires both protection from excess electrical influence of neighboring myocardial cells and unique action potential (AP) characteristics within the SAN cells. The latter includes spontaneous depolarization during diastole and a relatively slow rate of depolarization during the AP upstroke. These characteristics arise from a specific pattern of cardiac ion channel expression within SAN cells. SAN cells have i) very little inward rectifier (I_{K1}) [1–3], which in other cardiac cells holds the resting membrane potential around the K^+ equilibrium potential of −80/−90 mV and ii) pronounced hyperpolarization activated current (I_f), which activates at potentials as positive as −50 mV and initiates the slow diastolic depolarization of the membrane [4]; see also [5]. The combination of these two factors results in a less negative maximum diastolic potential (MDP) in SAN cells (−50 to −60 mV) than in extra-nodal cardiac cells. At these potentials, most of the sodium channels, even if present, are inactivated. Thus, unlike in working myocardium and Purkinje fibers, where Na current (I_{Na}) is responsible for the AP upstroke, the major contributor to the upstroke in typical SAN cells is the L-type Ca^{2+} current ($I_{Ca,L}$).

In addition to voltage dependent inactivation, diminished sodium channel expression also accounts for the reduced contribution of I_{Na} to the SAN AP. The absence of I_{Na} was demonstrated in adult rabbit primary pacemaker cells [6;7]. These cells are small in size, do not have striations and are mostly located in the center of the SAN [8;9]. Transitional cells located in the periphery have some atrial-like morphological and functional features and may exhibit a more robust I_{Na}. Consistent with these observations, tetrodotoxin (TTX) – sensitive APs were found in the periphery, but not in the center of the SAN [8;10]. Small rabbit SAN cells did not have I_{Na} while large cells did [11]. It is also possible that in those cases where I_{Na} was found in SAN cells with uncertain morphological and functional identification [12; 13], it could be attributed to transitional cells.

However, there are at least two examples where the existence of functional I_{Na} has been demonstrated in primary pacemaker cells of the SAN. It was shown that newborn rabbit SAN cells exhibit a prominent fast I_{Na} that contributes to the action potential upstroke [7] and diastolic depolarization [6]. In situ hybridization with anti-sense cDNA probes revealed the existence of the neuronal type I isoform of the sodium channel (Nav1.1) in newborn but not adult rabbit SAN cells [14]. High sensitivity of the newborn I_{Na} to TTX confirmed that the Na current did not arise from the cardiac Na channel isoform [14]. The more positive inactivation relation of the neuronal isoform, compared to that of the cardiac Na channel isoform, explains why these Na channels were not fully inactivated at the membrane potentials of the SAN.

More recently, I_{Na} was found in adult mouse SAN cells [1;15;16]. Using immunocytochemistry Lei et al. [15] revealed two sodium channel isoforms - neuronal Nav1.1 and cardiac Nav1.5; this finding was confirmed by Marionneau et al. [17]. The Nav1.1 isoform was distributed throughout the SAN, while Nav1.5 was only found in the periphery of the node. Lei et al. [15] were able to demonstrate existence of both TTX-sensitive and TTX-resistant components of I_{Na} in isolated mouse SAN cells, with TTX K_D values of 2.2 nmol/L and 0.4 μmol/L, respectively. Small cells (presumably from the center of the node) possessed both kinds of currents equally, while in large cells (presumably from the periphery) the density of TTX-resistant current was much greater. Significant contribution of TTX-sensitive I_{Na} to the control of spontaneous rate of isolated SAN cells [15] and of the whole mouse heart [18] was demonstrated.

The question that arises from the above findings relates to the role of functional I_{Na} in newborn rabbit and adult mouse SAN. In the rabbit, it was suggested that I_{Na} contributed to the higher

NIH-PA Author Manuscript

NIH-PA Author Manuscript

NIH-PA Author Manuscript

heart rates of the newborn and compensated for a positive shift of the L-type Ca current activation relation at that age [7;19]. Similarly, I_{Na} could be important for sustaining the high basal rate in adult small rodents such as the mouse. Alternatively, if persistent I_{Na} functionality is a more widespread feature of the adult mammalian SAN, it would have implications for future pharmacologic therapies for rhythm disorders. Data on the I_{Na} contribution to SAN function in a large mammalian heart, and the developmental regulation of any such current, has not previously been explored. However, neuronal ($Na_v1.1$, $Na_v1.2$, $Na_v1.3$) and cardiac ($Na_v1.5$) transcripts have been reported in dog SAN tissue [20]. We therefore asked if I_{Na} was present in the canine SAN, and if so, was it functional and was it developmentally regulated.

We found I_{Na} present at all ages in the canine SAN, with an age-dependent decrease in current magnitude. The current exhibited the highest TTX sensitivity in the adult, but at all ages the sensitivity was higher than would be expected from a pure cardiac channel isoform. Most important, the relatively negative position of the inactivation relation and absence of a significant "window" current suggest no functional role of I_{Na} in the physiological range of membrane potentials under normal conditions. However, computer simulations indicated that in the newborn, where the current is large, it could serve to protect against excess vagal slowing. Given that cardiac parasympathetic innervation precedes sympathetic innervation developmentally [21] there is potential for parasympathetic/sympathetic imbalance at young ages and thus a possible protective role of I_{Na}.

MATERIALS AND METHODS

Cell isolation

All procedures were performed according to the Guide for the Care and Use of Laboratory animals published by the US National Institutes of Health (Publication No. 85-23). Newborn (6–10 days old; NB), young (43–45 days old) and adult (1.5 years and older; AD) mongrel dogs were anesthetized with pentobarbital 30 mg/kg. The heart was removed and the right atrium with the right coronary artery was cut from the ventricle and placed in cold oxygenated Tyrode solution (in mmol/L: 140 NaCl, 5.4 KCl, 1 $CaCl_2$, 1 $MgCl_2$, 5 HEPES, 10 glucose; pH 7.4). In most cases, the sinus node artery was easily seen as a branch of the right coronary artery. In the newborn atrium, the right coronary artery was canulated toward the sinus node artery (SNA) with the canula tip close to the entry of the SNA. In young and adult dogs, the cut was made above the coronary artery and the canula inserted directly into the SNA. Blue dye diluted with Tyrode solution was injected to confirm perfusion of the SAN, located at the junction of the superior vena cava and right atrial free wall. The SNA, SAN, surrounding atrium and superior vena cava were isolated from the remainder of the atrium. All cut vessels leaking at the edges of the tissue were clamped. The tissue was perfused through the canula with 35° C Tyrode solution for 2–3 min, then with enzyme solution (in mmol/L: NaCl 140, KCl 5.4, $CaCl_2$ 0.2, $MgCl_2$ 0.5, taurine 50, HEPES 5, glucose 5.5, albumin 1 mg/ml, collagenase Worthington type 1 0.8–1.0 U/ml, protease 0.6 U/ml, elastase 1.9 U/ml; pH 6.9). After 5 min of enzyme perfusion, the SAN area and the tissue between the SAN and canula appeared swollen and slightly transparent. The swelling of the SAN zone after perfusion through the sinus node artery was described by James and Nadeau [22] in *in vivo* experiments with adult dogs; that swelling did not alter SAN function [22]. After 10–12 min of perfusing with enzyme solution, the tissue was cut into 2×2 mm pieces and triturated in 5 ml of fresh oxygenated enzyme solution of the same composition. After 15 min the solution was replaced by high K^+ solution (in mmol/L: L-glutamic acid 70, KOH 80, KCl 20, β-OH-buttiric acid sodium salt 10, KH_2 PO_4 10, HEPES-KOH 10, taurine 10, albumin 1 mg/ml; pH 7.4) and the tissue pieces were pipetted for 2–3 min for mechanical dissociation of cells. The solution was drawn off as the first fraction of isolated cells. Enzyme treatment of remaining tissue followed by pipetting in high K solution was repeated several times and 2–3 more fractions were collected. Usually

NIH-PA Author Manuscript

NIH-PA Author Manuscript

NIH-PA Author Manuscript

isolated cells were most abundant in the third fraction. The cells (see Fig 1E) were narrow and long (100–200 μm) and looked similar to dog SAN cells described previously [23]. They are also similar to “spindle” or “elongated spindle” SAN cells found in rabbits [24] and mice [16]. Most cells had striations which were more visible at the edges; in some cases a few tiny processes were visible. The adult cells were significantly larger than young and newborn cells (Table I). The cells were kept at 4–6°C for 2–20 hours until used experimentally. The final, fourth fraction had many short striated cells with numerous thick processes and was not used in this study.

Patch clamp experiments

Cells were placed in an experimental chamber and superfused with Tyrode solution. Membrane currents were recorded by whole cell patch clamp using a computer equipped with pCLAMP 8, a Digidata 1322A series interface and Axopatch 1C amplifier (Molecular Devices, Sunnyvale CA). Borosilicate glass pipettes (Sutter Instrument, Novato CA) were filled with a solution of the following composition (in mmol/L): NaCl 10, aspartic acid 80, CsOH 70, CsCl 40, $MgCl_2$ 2, EGTA 10, HEPES 10, ATP-Na 2, GTP-Na 0.1. Room temperature and reduced external Na^+ were used to reduce I_{Na}. After the membrane was ruptured and capacitance currents were compensated, the cell was superfused with a low- Na^+, Ca^{2+}- free solution (in mmol/L): NaCl 50, CsCl 5, tetraethyl-ammonium chloride 90, $MgCl_2$ 0.5, HEPES 10, glucose 5.5).

To study the I–V relationship, 50 ms test pulses were used from −80 mV to +40 mV with 10 mV intervals, preceded by a 500 ms prepulse to −110 mV. Holding potential between test episodes was −60 mV (see Fig 2). To study the effect of TTX (Calbiochem, San Diego CA) on I_{Na}, a single test pulse to −10 mV preceded by a 500 ms prepulse to −110 mV was repeated every 4 s. During a 40–60 s recording period, TTX was given at a single concentration (1, 10, 100, or 1000 nmol/L). If the current was completely restored after washout, a second higher concentration of TTX was given; no more than 2 concentrations of TTX were used on any cell. To study the voltage dependence of steady-state inactivation (availability), a 500 ms conditioning pulse was followed by a 50 ms test pulse to −10 mV. Conditioning pulses varied from −120 mV to −10 mV; holding potential was −60 mV with a 2 s inter-episode interval.

To study the contribution of I_{Na} to SAN pacemaking activity, spontaneous APs of SAN cells were recorded in current clamp mode. In this case the pipette solution contained (mmol/L): aspartic acid 130, KOH 146, NaCl 10, $CaCl_2$ 2, EGTA 5, HEPES 10, Mg ATP 2; pH 7.2. Spontaneous APs were recorded in Tyrode solution for 40–60 s, then the perfusate was changed for Tyrode solution containing 10 or 100 nmol/L TTX. To evaluate the chronotropic effect of TTX, cycle length values were obtained using the “pick peaks” tool of Origin 7 (OriginLab Corp, Northampton MA) and plotted against the time of recording.

Activation and inactivation were analyzed according to Boltzmann fitting analysis (Origin). Data are presented as mean ± SEM. Statistical significance was determined by ANOVA or Student’s t-test as appropriate. A value of $p<0.05$ was regarded as significant. The electrophysiological records were not corrected for junction potential, which in previous studies was found to be ~10 mV under these recording conditions.

Computer simulations

The SAN model of Kurata *et al* [25] was used, with the addition of a Na current Markov model fitted to amplitude and kinetics of experimentally obtained data in newborn and adult cardiac cells. Table S1 in the *online supplement* lists the parameters used to simulate the newborn and adult I_{Na}, while supplemental Figure S1 illustrates the calculated Na I–V relation at each age. Since we did not have complete data on all ionic currents in the canine SAN, or how they might

NIH-PA Author Manuscript

NIH-PA Author Manuscript

NIH-PA Author Manuscript

differ developmentally, we did not make any other modifications to the model of Kurata *et al*. To mimic vagal stimulation, we initially increased background inward rectifier current 4x. This was sufficient to hyperpolarize the maximum diastolic potential (MDP) 10 mV, approximating experimental reports of the effect of a high concentration of acetylcholine [26]. Effects of vagal stimulation on other currents were also simulated, as indicated in the text.

RESULTS

Identification of pacemaker cells

To confirm the pacemaker origin of the isolated cells, the pacemaker current (I_f) was recorded from newborn and adult cells using a series of hyperpolarizing pulses (−45 to −105 mV from holding potential of −35 mV). Normal Tyrode solution and the solution for AP recordings (see Methods) were used as the bath and pipette solutions respectively. As shown in Fig 1, typical slowly activating currents were observed beginning with voltage steps as negative as −55 mV. At −105 mV the current density ranged from 8 – 17 pA/pF (Table I), which is comparable to the approximate 15–16 Pa/pF value of rabbit [27] or murine [16] SAN cells. Further, the adult and newborn IV relations were significantly different (ANOVA), which is qualitatively similar to the reported age-dependent change in I_f current density in the rabbit SAN [27]. When the IV relations were converted to activation relations with a Boltzmann function, midpoint did not differ with age (Table I).

In addition, APs were recorded from spontaneously beating adult cells and the MDP, the threshold potential for phase 0, the peak amplitude and maximal dV/dt of the AP upstroke (V_{max}) were measured. A representative train of APs is shown in Fig 1D. The APs had the typical SAN AP shape, with relatively positive MDP (−53.2 ±2.1 mV, n=12), prominent diastolic depolarization with a mean AP threshold potential of −41.9±1.6 mV (n=12) and slow phase 0 (V_{max} 2.2±0.2 V/s, n=12). The mean peak amplitude was 76.3 ±3.7 mV (n=12). The low value for V_{max} suggests these are not Na-dependent APs.

Na current activation

In a reduced Na^+, Ca^{2+}-free solution, fast and quickly inactivated inward currents were observed with depolarizing steps from a conditioning pulse to test potentials positive to −60 mV. Such a current was seen in 93.2%, 94.1%, and 81.8% of cells from adult, young and newborn animals, respectively. Thus, unlike our prior study in the rabbit, in the canine SAN a Na current persists during post-natal development. However, as detailed below, some characteristics of the current were developmentally regulated.

Unlike adult and young cells, newborn SAN cells did not tolerate repeated hyperpolarizing pulses to −110 mV. Therefore, a holding potential of −90 mV was used instead of prepulses to −110 mV to construct I–V curves for newborn SAN cells. As discussed below, about half the current may be lost because of partial inactivation at −90 mV. However the shape of the activation relation should not be affected by this inactivation. Fig 2 shows original traces of the current recorded from a young SAN cell and average I–V curves for all three ages. The current in NB cells is much larger than in young and adult cells ($p=<0.001$ for both comparisons, ANOVA), despite being recorded from a less negative holding potential that would tend to underestimate the magnitude. The current in young cells also is larger than in adult ($p = 0.004$, ANOVA), so that there is a progressive reduction in current density with age. In all age groups the current threshold was around −60 mV and current density reached a maximum at −20 mV. All activation curves were parallel to each other (Fig 2D). Small differences in midpoint and slope were not statistically significant (Table I).

NIH-PA Author Manuscript

NIH-PA Author Manuscript

NIH-PA Author Manuscript

Na current inactivation

Fig 3 shows the voltage-dependence of steady-state inactivation of the Na current. Curves for adult and NB cells are parallel and have almost identical voltage dependence. Half-inactivation voltages are −89.7±0.7 mV, −95.1 ± 1.2 mV and −93.4 ± 1.9 mV for NB, young, and AD, respectively. The curve for NB cells is slightly shifted in the positive direction, with midpoint statistically different from that of the young group, but not from adult (Table I). The difference in slope values is statistically insignificant. Fig 3 also illustrates the minimal "window currents" for all three age groups.

Effect of TTX on I_{Na}

In the newborn rabbit SAN, the Na current is due to expression of a neuronal isoform [14], which has greater TTX sensitivity than the typical cardiac isoform (Na1.5) prevalent in the ventricle. We therefore investigated the TTX sensitivity of the canine SAN Na current as a function of age. Fig 4 shows the effect of TTX on I_{Na} produced by single pulses to −10 mV given every 4 s. TTX dose-dependently reduced the current in all three ages. The effect was age-dependent, with AD cells being more sensitive to TTX than young or NB ones (Fig 4B and 4C), suggesting that although the current is smallest in the AD, it may contain the least "contamination" by the cardiac isoform. The limited number of TTX concentrations used for these experiments does not allow construction of full concentration-effect curves to obtain accurate IC50 values. However the difference is apparent when looking at the effect of 100 nmol/L TTX. At this dose, current is inhibited 47±7, 60±4 and 91±3% in NB, young and AD cells, respectively (Table I). In the adult, in particular, the IC50 value is on the order of 10 nmol/L TTX or less.

The combination of a relatively negative inactivation relation and a high sensitivity to TTX is unusual, since the neuronal and skeletal Na channel isoforms that exhibit high TTX sensitivity are reported to inactivate at less negative potentials [28]. In a separate group of AD SAN cells we therefore determined the effect of 10 nmol/L TTX on the midpoint of inactivation. We reasoned that if the net Na current reflected a mix of TTX-sensitive but positive inactivating and TTX-insensitive but negative inactivating isoforms, then such a low dose of TTX would selectively inhibit the TTX-sensitive isoform and shift inactivation more negative. In 7 cells, the peak current for a step to −120 mV was reduced 40% by 10 nmol/L TTX, but midpoint of inactivation was not affected (−90.0 mV in control vs −91.3 mV after TTX). Thus, the TTX sensitive component of I_{Na} exhibits a relatively negative inactivation relation in the AD canine SAN cells.

Effect of TTX on cycle length

The measured inactivation relation, combined with the recorded MDP and V_{max}, suggest that the Na channels will not be available during normal spontaneous activity. As illustrated in Fig 5, TTX did not change cycle length of spontaneous APs in adult SAN. In experiments with 10 nmol/L TTX, a concentration that inhibited the Na current by about 2/3 in adult SAN, the cycle length before and after TTX was 1561±217 and 1608±1244 ms respectively (n=3), and corresponding values for experiments with 100 nM TTX (which blocked ~90% of current) were 1684±1523 and 1687±1491 ms (n = 5). Other AP parameters (MDP, take-off potential, AP overshoot, V_{max}) also were unaffected by TTX, again indicating the channels are not functionally available at the normal voltages of the adult SAN cell.

Simulation of effect of vagal stimulation in the presence and absence of Na current

Given the negative inactivation relation of I_{Na} at all ages in the canine SAN, if the current is to contribute to automaticity it would only be under conditions where the cells are markedly hyperpolarized, such as during strong vagal stimulation. This could occur in the newborn,

NIH-PA Author Manuscript

NIH-PA Author Manuscript

NIH-PA Author Manuscript

where a parasympathetic/sympathetic imbalance might result from the differing developmental time course of parasympathetic and sympathetic innervation of the heart [21]. Further, the larger Na current at this age increases the likelihood of such a contribution. Since we were not able to record APs from the fragile newborn SAN cells, we turned to a computer model to evaluate the possibility that strong vagal stimulation could recruit Na current. Fig. 6 illustrates the results of adding a newborn- or adult-like Na current to an existing SAN model, incorporating our experimental data from newborn and adult canine SAN cells. Under normal conditions, there is no effect on spontaneous rate of adding either the newborn or adult I_{Na} to the model. When background K conductance is increased 4x to cause a 10 mV hyperpolarization (to approximate the effect of Ach [26]), rate slows regardless of the presence or absence of Na current. However, rate slows somewhat less with inclusion of the much larger NB current. When stronger vagal stimulation is mimicked by increasing background K conductance 5x, spontaneous activity ceases in the normal model and in the AD Na current model. In contrast, automaticity persists, albeit at a slower rate, in the presence of the NB Na current. In a separate simulation, we included a 10 mV negative shift of pacemaker current activation and a 10% reduction of L-type Ca current amplitude to mimic additional effects of strong vagal stimulation (data not shown). Slowing was greater in each case but the same qualitative effect was observed of protection only with the NB I_{Na} parameters.

Fig. 7 further illustrates the effect of membrane hyperpolarization on the contribution of I_{Na} to the newborn AP. We simulated spontaneous APs (top) and the underlying Na current (bottom) in the newborn model under control conditions and when background K conductance is increased 4x and 5x. The results show a progressively larger Na current contribution to diastole and AP upstroke as the membrane K conductance increases. Thus, the presence of a Na current with a negative inactivation relation is protective under hyperpolarizing conditions, but the effect is strongly dependent on the magnitude of the current and the degree of hyperpolarization.

DISCUSSION

Several new findings resulted from this study: i) At all ages, most canine SAN cells have I_{Na}, and the current is more sensitive to TTX than would be expected from the cardiac isoform alone. ii) The current density decreases developmentally, but at the same time the TTX sensitivity of the remaining current increases, suggesting disproportionate loss of a TTX-insensitive component. iii) The relatively negative voltage range for inactivation results in complete inactivation and unavailability of the current at the typical SAN MDP for all ages. iv) Under conditions of membrane hyperpolarization such as strong vagal activation, the large newborn I_{Na} becomes available and can serve to protect against excess slowing or cessation of rate.

The present study was undertaken to prove or reject the hypothesis that while I_{Na} plays a significant role in pacemaking in small animals like adult mice [15] or newborn rabbits [6;7], which normally have faster heart rates than larger animals, it does not have such a contribution in larger animals like the dog or adult rabbit (and probably human). Our results confirmed the absence of a functional contribution of the current in the adult canine SAN, but unexpectedly found that this was due to inactivation of the channel rather than its absence. We therefore proceeded to test the possibility that the unavailable Na channels are recruited to help maintain excitability under conditions of membrane hyperpolarization. This could occur in peripheral regions of the node, where the cells are in direct electrical contact with atrial myocardium. In addition, since parasympathetic innervation reaches the heart first during development [21], it is possible that there could be periods of excess vagal tone prior to maturity. If this results in marked hyperpolarization, the silent Na channels could serve a protective role maintaining automaticity. This is particularly likely to occur in the newborn, both because that is the time

NIH-PA Author Manuscript

NIH-PA Author Manuscript

NIH-PA Author Manuscript

period where such autonomic imbalance is plausible, and because the current is markedly larger at this age. Our computer simulation supports this conclusion. Further, since the youngest age studied was 6 days postpartum, we cannot exclude the possibility that at even younger ages, including in the fetus when heart rate is faster than in the newborn, I_{Na} contributes more directly to SAN pacemaking.

Aspects of our findings have both similarities and differences to what has been reported in the two other species where SAN Na current has been studied developmentally, the rabbit and mouse. For example, the age-dependent decrease of current parallels what has been reported in rabbit SAN [7], while the persistence of a TTX-sensitive current in the adult is reflective of what has been reported in the mouse SAN [15]. However, while the high TTX sensitivity suggests the contribution of neuronal or skeletal Na channel isoforms in the canine SAN, the inactivation relation is more negative than that reported for any of these isoforms in heterologous systems. As a result, unlike in rabbit or murine SAN, the Na current does not contribute to normal automaticity or AP generation in the canine SAN at any post-natal age, and likely plays a role only during strong vagal stimulation, particularly in the newborn. In contrast to our findings in the canine SAN, in the newborn (but not adult) rabbit SAN the Na current (Nav1.1 [14]) has a relatively positive inactivation relation that permits Na channel availability at normal diastolic potentials. This results in a contribution to diastolic depolarization, AP upstroke and spontaneous rate because the newborn rabbit Na channels exhibit frequent re-openings at diastolic potentials, resulting in complete but slow inactivation. That is, current flows during diastole due to the kinetic properties of the channel rather than the presence of a steady-state window current at diastolic potentials [6;7;29]. It remains to be determined if a similar mechanism applies in the newborn canine SAN during membrane hyperpolarization.

While in the rabbit SAN there appears to be an age-dependent loss of Nav1.1, in the whole murine heart, all Na channel transcripts increase during the postnatal period, but TTX-sensitive neuronal $Na_v1.1$–$Na_v1.3$ and skeletal $Na_v1.4$ Na channel transcripts increase more significantly than $Na_v1.5$ [30;31]. In adult animals, Nav1.5 and $Na_v1.1$ play an important role in pacemaking. As was shown by [15], both isoforms participate in initiation of the AP, while $Na_v1.5$, but not $Na_v1.1$ provides propagation of APs from the center to periphery. We did not attempt to molecularly identify the Na channel isoforms present in the canine SAN in this study, but this has previously been addressed in the adult canine SAN [20], which expresses transcripts for $Na_v1.5$ and neuronal isoforms ($Na_v1.1$, $Na_v1.2$, and $Na_v1.3$) in an approximate 4:1 ratio. Among neuronal transcripts, the amount of $Na_v1.3$ is the greatest, in comparison to the other isoforms studied. Based on the high TTX sensitivity we observed in adult canine SAN (IC50 < 10 nmol/L), we would expect $Na_v1.5$ to represent far less than 80% of the total available Na channels (the 4:1 ratio observed at the transcript level for the specific isoforms measured).

I_{Na} of adult dog SAN cells is as sensitive to TTX as neuronal or skeletal isoforms [32;33]but inactivates at more negative potentials [28]. Activation and inactivation properties of Na channel isoforms are influenced by intracellular environment [34], but there is no precedent for the very negative position of the inactivation relation found in this study. While the molecular basis of the negative inactivation in the canine SAN remains to be determined, the result is that the current does not contribute to normal electrophysiological activity in the isolated cells. At all post-natal ages studied the current is completely inactivated by −70 mV. Considering the mean MDP recorded in adult SAN cells (−53 mV), there should not be any available I_{Na}. This is in agreement with experimental results, where TTX did not have any effect on spontaneous APs of adult SAN cells. Moreover, the AP shape, with its shallow upstroke and rounded peak, further argues against a contribution of I_{Na}. The V_{max} value in our experiments (2.2 V/s) was very close to the value for adult rabbit SAN cells also obtained at

NIH-PA Author Manuscript

NIH-PA Author Manuscript

NIH-PA Author Manuscript

room temperature (2.6 ± 0.8 V/s [7]). Based on the inactivation relation and computer simulation, one can expect the same result in NB SAN cells.

Although our data do not support a direct role of Na current during normal automaticity within isolated canine SAN cells, this should not be interpreted to imply that Na channel disruptions in large mammals or humans cannot influence SAN function. Clinical studies demonstrate that sodium channelopathies due to mutations in either TTX-insensitive [35] or TTX-sensitive [36] Na channel isoforms may result in abnormalities of SAN performance. However, this effect need not arise from channels localized to the central SAN, as effects at the periphery or in the atrial tissue into which the impulse propagates could play a role. In addition, a recent study on a small number of isolated human SAN cells found evidence for the presence of I_{Na} [37]. Since the current, which was seen at −70 mV and more negative potentials, completely disappeared at −60 mV, it is uncertain if the current would be available at the approximately −65 mV MDP of these cells, but it could well be available during situations such as vagal stimulation that result in membrane hyperpolarization. Therefore, like in the case of dog SAN, the functional role of I_{Na} in human SAN cells requires further study.

Supplementary Material

Refer to Web version on PubMed Central for supplementary material.

Acknowledgments

GRANTS

This work was supported by NIH program project grant HL-28958 to R.B.R. and from the American Heart Association, National Institutes of Health NHLBI RO1-HL-085592 and Alfred P. Sloan Foundation to C.E.C.

REFERENCES

1. Cho HS, Takano M, Noma A. The electrophysiological properties of spontaneously beating pacemaker cells isolated from mouse sinoatrial node. J Physiol 2003;550(1):169–180. [PubMed: 12879867]
2. Irisawa H, Brown HF, Giles W. Cardiac pacemaking in the sinoatrial node. Physiol Rev 1993;73(1): 197–227. [PubMed: 8380502]
3. Noma A, Nakayama T, Kurachi Y, Irisawa H, Resting K. conductances in pacemaker and non-pacemaker heart cells of the rabbit. Jpn J Physiol 1984;34(2):245–254. [PubMed: 6088872]
4. DiFrancesco D, Ferroni A, Mazzanti M, Tromba C. Properties of the hyperpolarizing-activated current (if) in cells isolated from the rabbit sino-atrial node. J Physiol 1986;377:61–88. [PubMed: 2432247]
5. Baruscotti M, DiFrancesco D. Pacemaker channels. Ann NY Acad Sci 2004;1015(1):111–121. [PubMed: 15201153]
6. Baruscotti M, DiFrancesco D, Robinson RB. Na^+ current contribution to the diastolic depolarization in newborn rabbit SA node cells. Am J Physiol 2000;279(5):H2303–H2309.
7. Baruscotti M, DiFrancesco D, Robinson RB. A TTX-sensitive inward sodium current contributes to spontaneous activity in newborn rabbit sino-atrial node cells. J Physiol 1996;492(Pt 1):21–30. [PubMed: 8730579]
8. Boyett MR, Honjo H, Kodama I. The sinoatrial node, a heterogeneous pacemaker structure. Cardiovascular Research 2000;47(4):658–687. [PubMed: 10974216]
9. Opthof T, de Jonge B, Mackaay AJ, Bleeker WK, Masson-Pevet M, Jongsma HJ, et al. Functional and morphological organization of the guinea-pig sinoatrial node compared with the rabbit sinoatrial node. J Mol Cell Cardiol 1985;17(6):549–564. [PubMed: 4020878]
10. Kodama I, Nikmaram MR, Boyett MR, Suzuki R, Honjo H, Owen JM. Regional differences in the role of the Ca^{2+} and Na^+ currents in pacemaker activity in the sinoatrial node. Am J Physiol 1997;272 (6 Pt 2):H2793–H2806. [PubMed: 9227559]

NIH-PA Author Manuscript

NIH-PA Author Manuscript

NIH-PA Author Manuscript

11. Honjo H, Boyett MR, Kodama I, Toyama J. Correlation between electrical activity and the size of rabbit sino-atrial node cells. J Physiol 1996;496(3):795–808. [PubMed: 8930845]
12. Muramatsu H, Zou AR, Berkowitz GA, Nathan RD. Characterization of a TTX-sensitive Na^+ current in pacemaker cells isolated from rabbit sinoatrial node. Am J Physiol 1996;270(6):H2108–H2119. [PubMed: 8764263]
13. Nathan RD. Two electrophysiologically distinct types of cultured pacemaker cells from rabbit sinoatrial node. Am J Physiol 1986;250(2 Pt 2):H325–H329. [PubMed: 3946631]
14. Baruscotti M, Westenbroek R, Catterall WA, DiFrancesco D, Robinson RB. The newborn rabbit sino-atrial node expresses a neuronal type I-like Na^+ channel. J Physiol 1997;498(3):641–648. [PubMed: 9051576]
15. Lei M, Jones SA, Liu J, Lancaster MK, Fung SSM, Dobrzynski H, et al. Requirement of neuronal- and cardiac-type sodium channels for murine sinoatrial node pacemaking. J Physiol 2004;559(3): 835–848. [PubMed: 15254155]
16. Mangoni M, Nargeot J. Properties of the hyperpolarization-activated current (If) in isolated mouse sino-atrial cells. Cardiovasc Res 2001;52(1):51–64. [PubMed: 11557233]
17. Marionneau C, Couette B, Liu J, Li H, Mangoni ME, Nargeot J, et al. Specific pattern of ionic channel gene expression associated with pacemaker activity in the mouse heart. J Physiol 2005;562(1):223–234. [PubMed: 15498808]
18. Maier SKG, Westenbroek RE, Yamanushi TT, Dobrzynski H, Boyett MR, Catterall WA, et al. An unexpected requirement for brain-type sodium channels for control of heart rate in the mouse sinoatrial node. PNAS 2003;100(6):3507–3512. [PubMed: 12631690]
19. Protas L, DiFrancesco D, Robinson RB. L-type but not T-type calcium current changes during postnatal development in rabbit sinoatrial node. Am J Physiol 2001;281(3):H1252–H1259.
20. Haufe V, Cordeiro JM, Zimmer T, Wu YS, Schiccitano S, Benndorf K, et al. Contribution of neuronal sodium channels to the cardiac fast sodium current I_{Na} is greater in dog heart Purkinje fibers than in ventricles. Cardiovasc Res 2005;65(1):117–127. [PubMed: 15621039]
21. Robinson RB, Yu H, Chang F, Cohen IS. Developmental change in the voltage-dependence of the pacemaker current, if, in rat ventricle cells. Pflugers Archiv 1997;433(4):533–535. [PubMed: 9000433]
22. James TN, Nadeau Reginald A. Direct perfusion of the sinus node: an experimental model for pharmacologic and electrohpysiologic studies of the heart. Henry Ford Hosp.Med.Bull 1962;10(pt 1):21–25. [PubMed: 14451022]
23. Kwong KF, Schuessler RB, Green KG, Laing JG, Beyer EC, Boineau JP, et al. Differential expression of gap junction proteins in the canine sinus node. Circ Res 1998;82(5):604–612. [PubMed: 9529165]
24. Verheijck EE, Wessels A, van Ginneken AC, Bourier J, Markman MW, Vermeulen JL, et al. Distribution of atrial and nodal cells within the rabbit sinoatrial node: models of sinoatrial transition. Circulation 1998;97(16):1623–1631. [PubMed: 9593568]
25. Kurata Y, Hisatome I, Imanishi S, Shibamoto T. Dynamical description of sinoatrial node pacemaking: improved mathematical model for primary pacemaker cell. Am J Physiol 2002;283 (5):H2074–H2101.
26. Campbell GD, Edwards FR, Hirst GD, O'Shea JE. Effects of vagal stimulation and applied acetylcholine on pacemaker potentials in the guinea-pig heart. J Physiol 1989;415(1):57–68. [PubMed: 2640469]
27. Accili EA, Robinson RB, DiFrancesco D. Properties and modulation of If in newborn versus adult cardiac SA node. Am J Physiol 1997;272(3 Pt 2):H1549–H1552. [PubMed: 9087633]
28. Catterall WA, Goldin AL, Waxman SG. International Union of Pharmacology. XLVII. Nomenclature and structure-function relationships of voltage-gated sodium channels. Pharmacol Rev 2005;57(4): 397–409. [PubMed: 16382098]
29. Baruscotti M, DiFrancesco D, Robinson RB. Single-channel properties of the sinoatrial node Na+ current in the newborn rabbit. Pflugers Arch 2001;442(2):192–196. [PubMed: 11417213]
30. Haufe V, Camacho JA, Dumaine R, Gunther B, Bollensdorff C, von Banchet GS, et al. Expression pattern of neuronal and skeletal muscle voltage-gated Na^+ channels in the developing mouse heart. J Physiol 2005;564(3):683–696. [PubMed: 15746173]

NIH-PA Author Manuscript

NIH-PA Author Manuscript

NIH-PA Author Manuscript

31. Maier SKG, Westenbroek RE, McCormick KA, Curtis R, Scheuer T, Catterall WA. Distinct subcellular localization of different sodium channel alpha and beta subunits in single ventricular myocytes from mouse heart. Circulation 2004;109(11):1421–1427. [PubMed: 15007009]

32. Goldin AL. Resurgence of sodium channel research. Ann Rev Physiol 2001;63(1):871–894. [PubMed: 11181979]

33. Meadows LS, Chen YH, Powell AJ, Clare JJ, Ragsdale DS. Functional modulation of human brain Nav1.3 sodium channels, expressed in mammalian cells, by auxiliary [beta]1, [beta]2 and [beta]3 subunits. Neuroscience 2002;114(3):745–753. [PubMed: 12220575]

34. Cummins TR, Aglieco F, Renganathan M, Herzog RI, Dib-Hajj SD, Waxman SG. Nav1.3 Sodium channels: rapid repriming and slow closed-state inactivation display quantitative differences after expression in a mammalian cell line and in spinal sensory neurons. J Neurosci 2001;21(16):5952–5961. [PubMed: 11487618]

35. Veldkamp MW, Wilders R, Baartscheer A, Zegers JG, Bezzina CR, Wilde AAM. Contribution of sodium channel mutations to bradycardia and sinus node dysfunction in LQT3 families. Circ Res 2003;92(9):976–983. [PubMed: 12676817]

36. Haufe V, Chamberland C, Dumaine R. The promiscuous nature of the cardiac sodium current. J Mol Cell Cardiol 2007;42(3):469–477. [PubMed: 17289073]

37. Verkerk A, Wilders R, van Borren M, Tan H. Is sodium current present in human sinoatrial node cells? Int J Biol Sci 2009;5(2):201–204. [PubMed: 19240810]

NIH-PA Author Manuscript
NIH-PA Author Manuscript
NIH-PA Author Manuscript

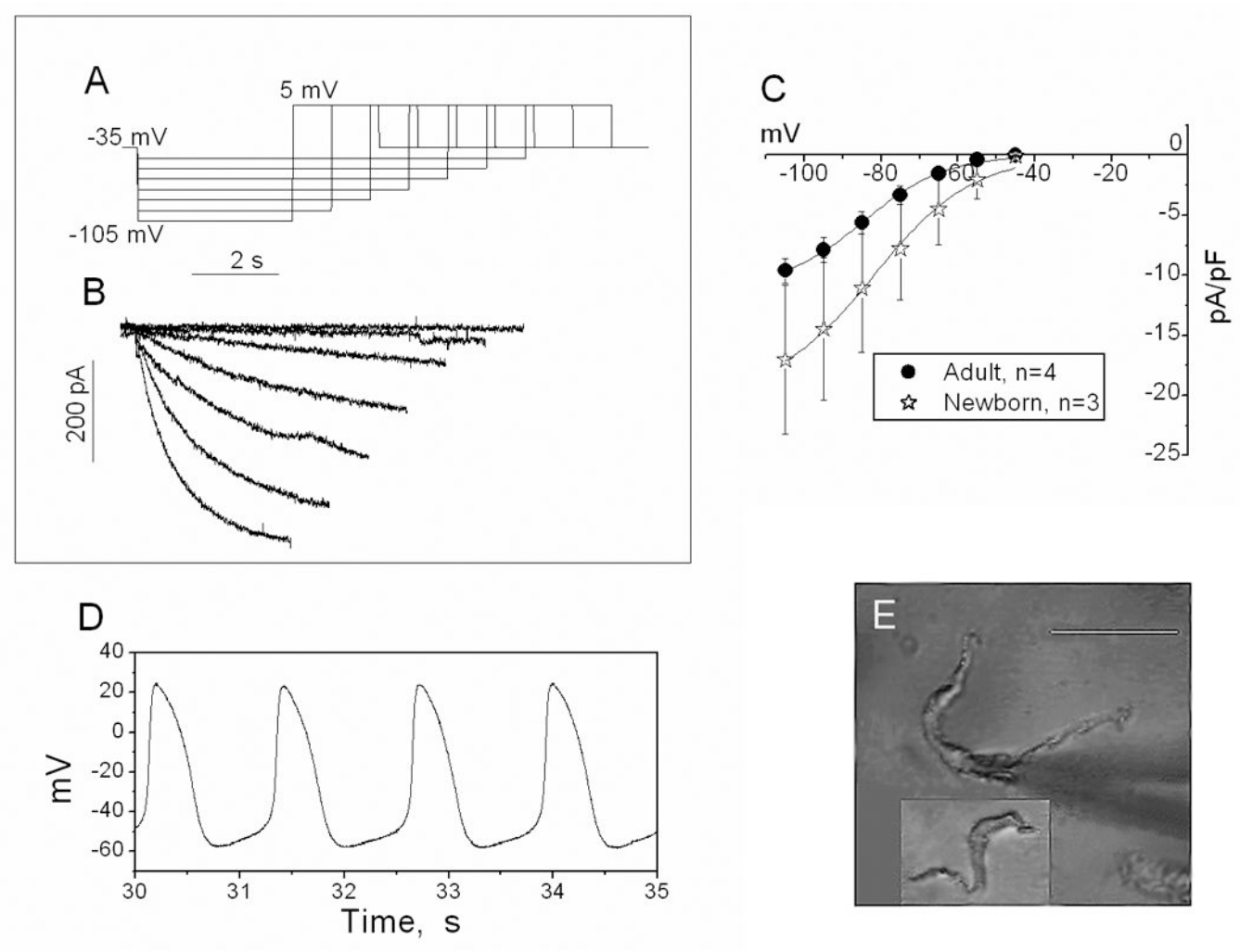

Figure 1. Hyperpolarization-activated current (I_f) and action potentials

A. Voltage steps used to produce I_f (from −45 mV to −105 mV) followed by a step to +5 mV to deactivate I_f. Holding potential −35 mV. **B**. Representative current traces recorded from a newborn (9-day old) SAN cell. Only inward currents are shown. Values at the end of the traces were used to construct I–V curves. **C**. Mean I–V curves for I_f obtained from adult and newborn SAN cells; the 2 curves significantly differ by ANOVA. **D**. Typical recording of APs of an adult SAN cell at 20°C; note a prominent diastolic depolarization and shallow AP upstroke. **E**. Photographs of adult and newborn (in the box) SAN cells. Scale bar: 50 microns.

NIH-PA Author Manuscript
NIH-PA Author Manuscript
NIH-PA Author Manuscript

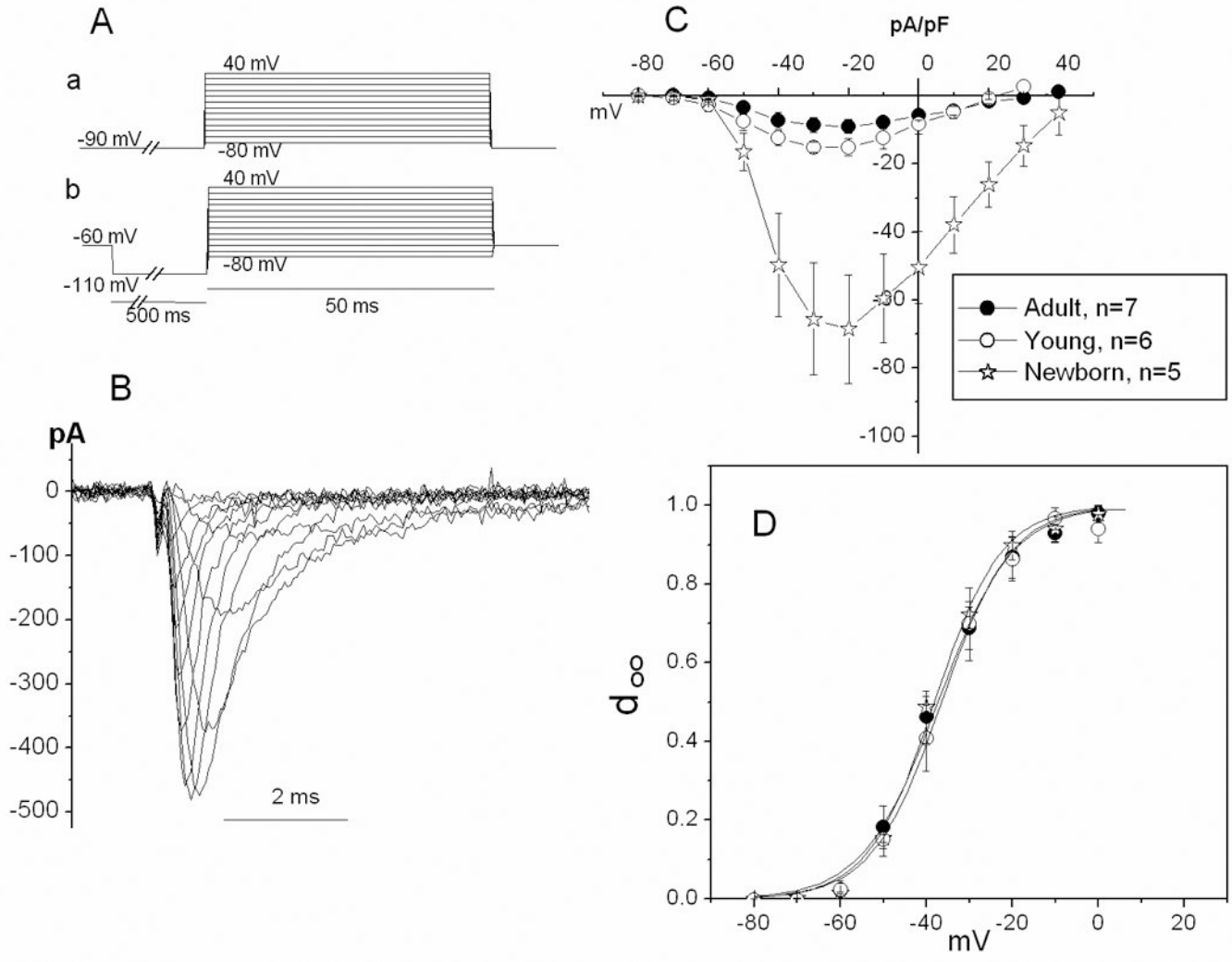

Figure 2. Age-dependence of I_{Na} I–V and activation relations

A. Waveform configuration (see Methods) for recording I_{Na}. a and b: protocols used in experiments with newborn (a) or adult and young (b) animals (see Methods). **B**. Family of traces of I_{Na} recorded from an SAN cell from a 40 day old dog (young group). **C**. Mean I–V curves for three ages. **D**. Activation curves for three ages. Activation variable (d_∞) was calculated as g/g_{max}. To determine g values, reversal potential for I_{Na} was estimated as the potential at which the extrapolation of the right limb of the I–V curve crossed the voltage axis; n values are the same as in C.

NIH-PA Author Manuscript
NIH-PA Author Manuscript
NIH-PA Author Manuscript

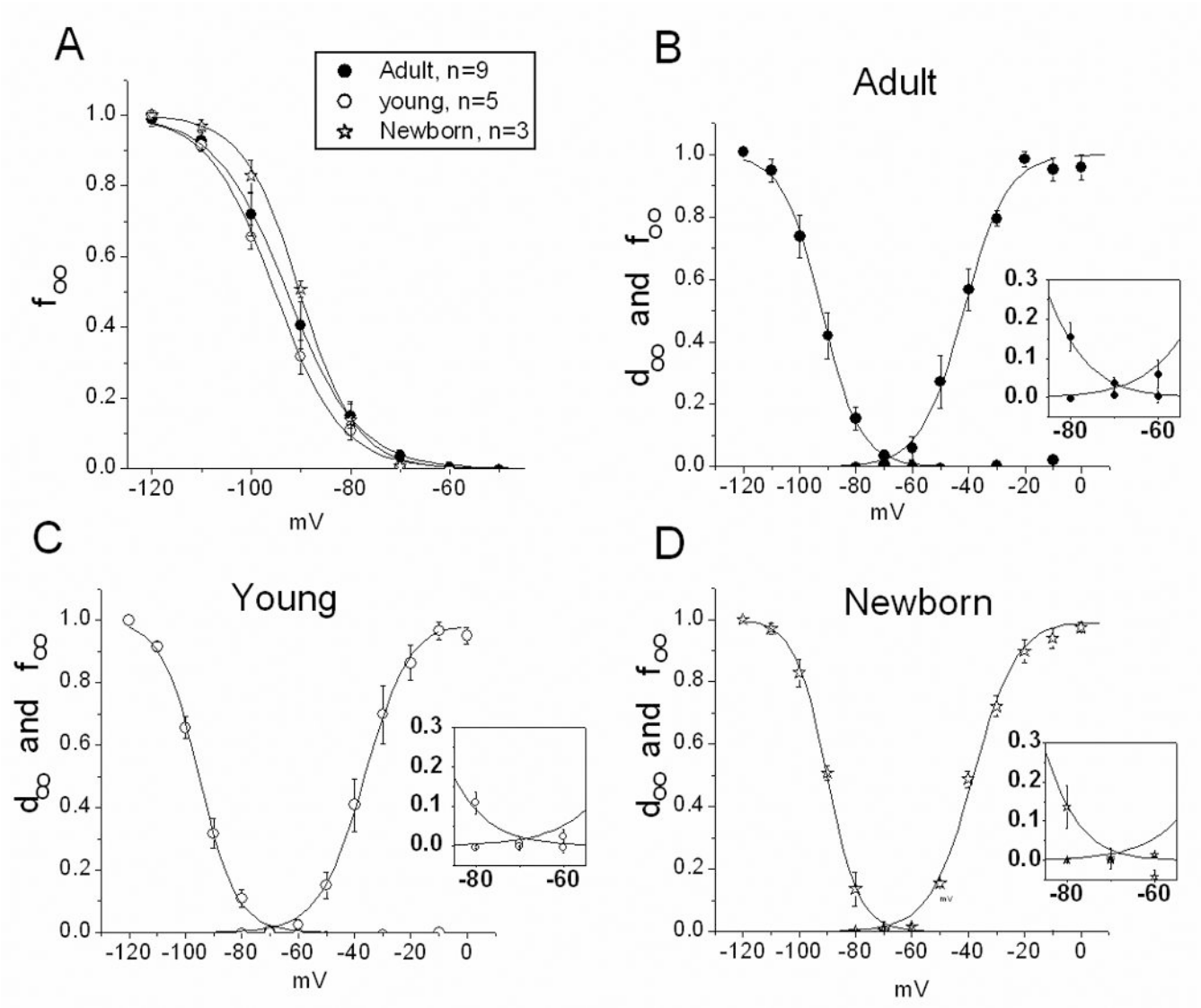

Figure 3. I_{Na} activation and inactivation relations

A. Inactivation variable (f_∞) for three age groups. **B, C** and **D**. Activation (d_∞) and inactivation variables plotted together. *Insets:* Expansion of the middle portion of curves to illustrate the minimal 'window" current for all groups. For n in activation curves, see Figure 2.

NIH-PA Author Manuscript

NIH-PA Author Manuscript

NIH-PA Author Manuscript

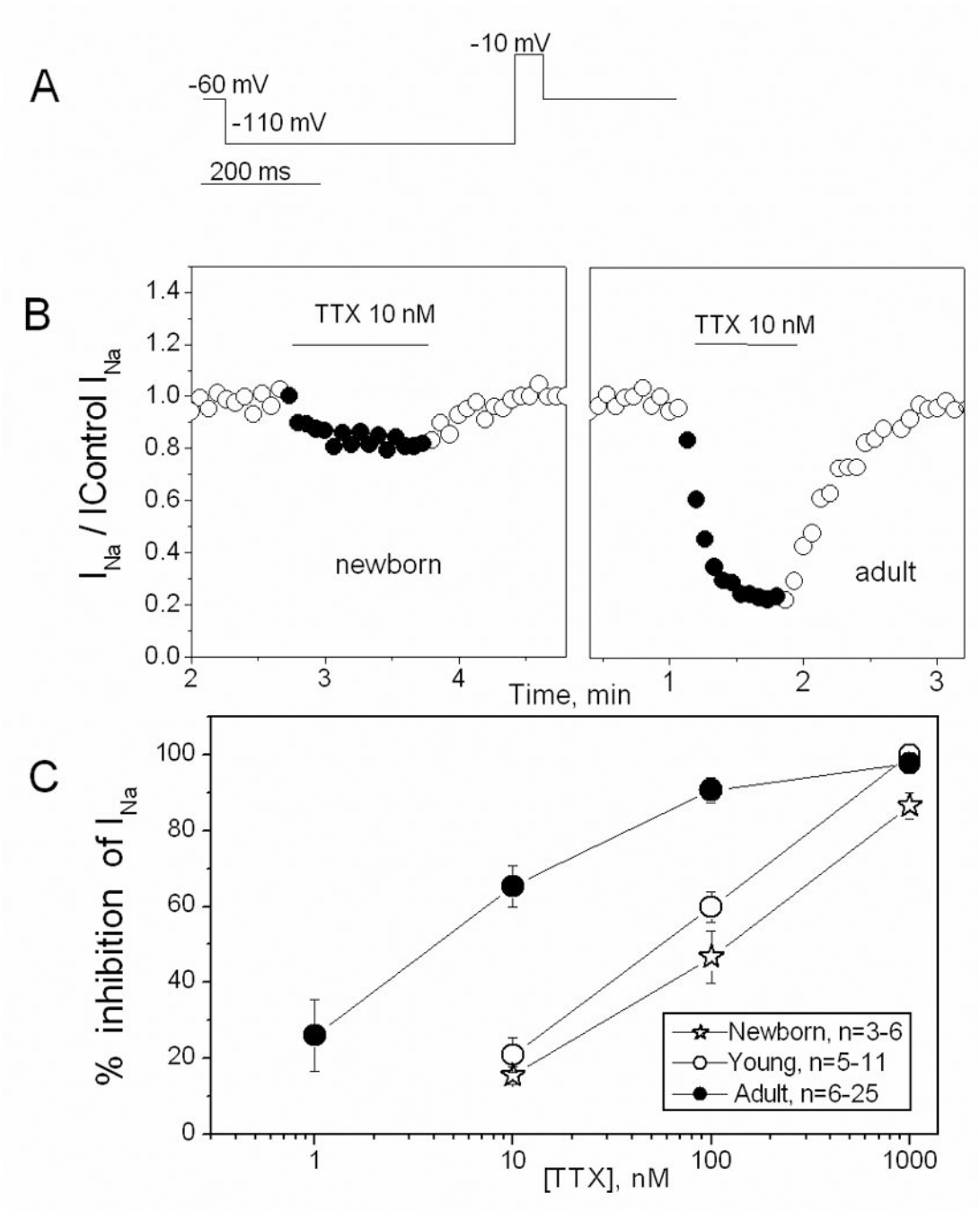

Figure 4. TTX sensitivity of I_{Na}

A. Single step voltage protocol used to elicit I_{Na}. **B.** Time course of the effect of 10 nmol/L TTX on I_{Na} in newborn (left panel) and adult (right panel) SAN cells, illustrating the more pronounced effect in the adult. Values of the current are normalized to the control values. **C.** TTX concentration-effect curves for 3 ages.

NIH-PA Author Manuscript

NIH-PA Author Manuscript

NIH-PA Author Manuscript

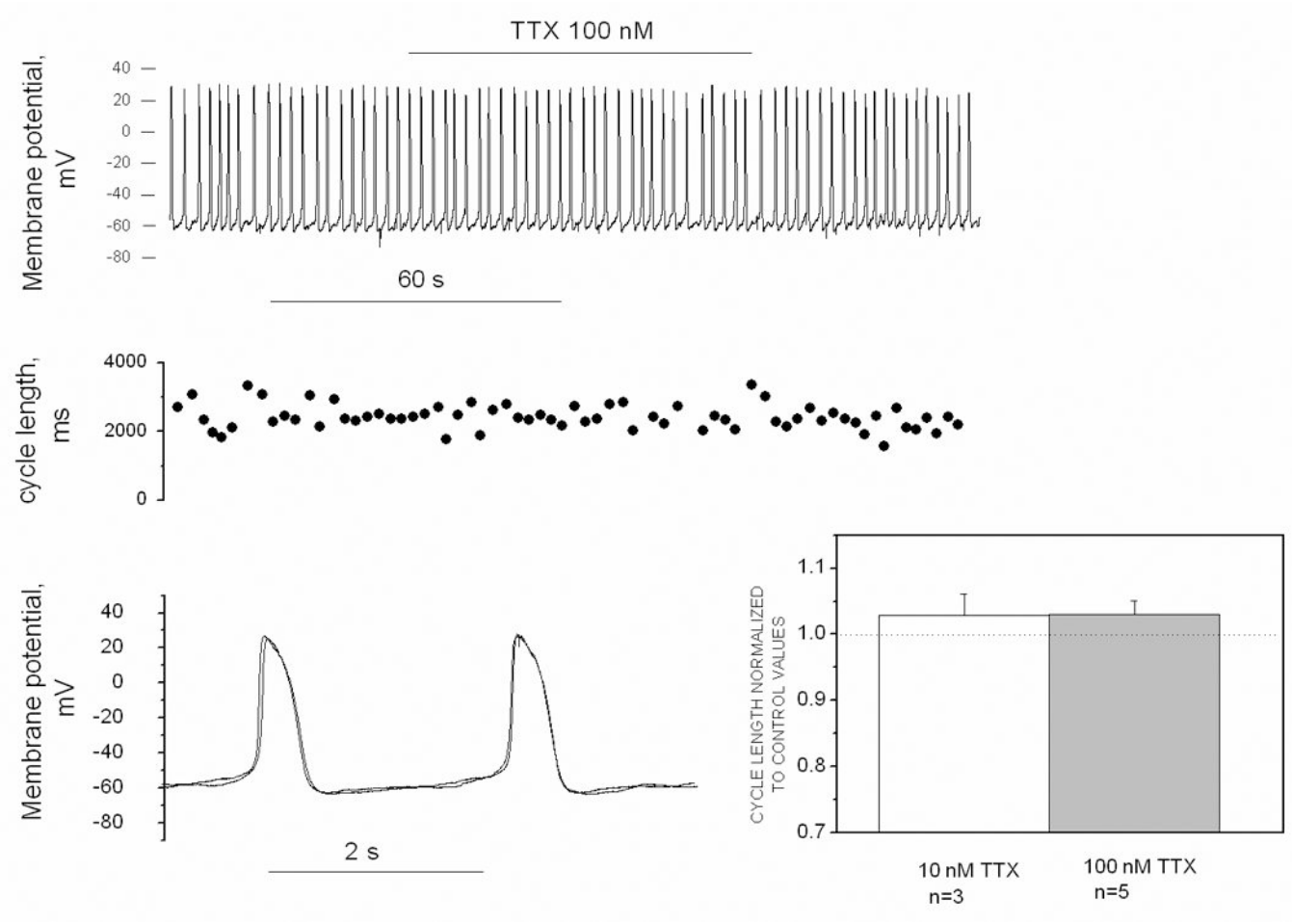

Figure 5. Effect of TTX on action potential

A. Original traces of membrane potential recorded in current clamp mode from an adult SAN cell. **B.** Cycle length of APs presented in the pane Al. **C.** Superimposed APs from panel A taken before and during TTX application. **D.** Mean cycle length values in the presence of 10 nM and 100 nM TTX, normalized to control values. The difference from the control level (dash line) is not statistically significant at either concentration.

NIH-PA Author Manuscript

NIH-PA Author Manuscript

NIH-PA Author Manuscript

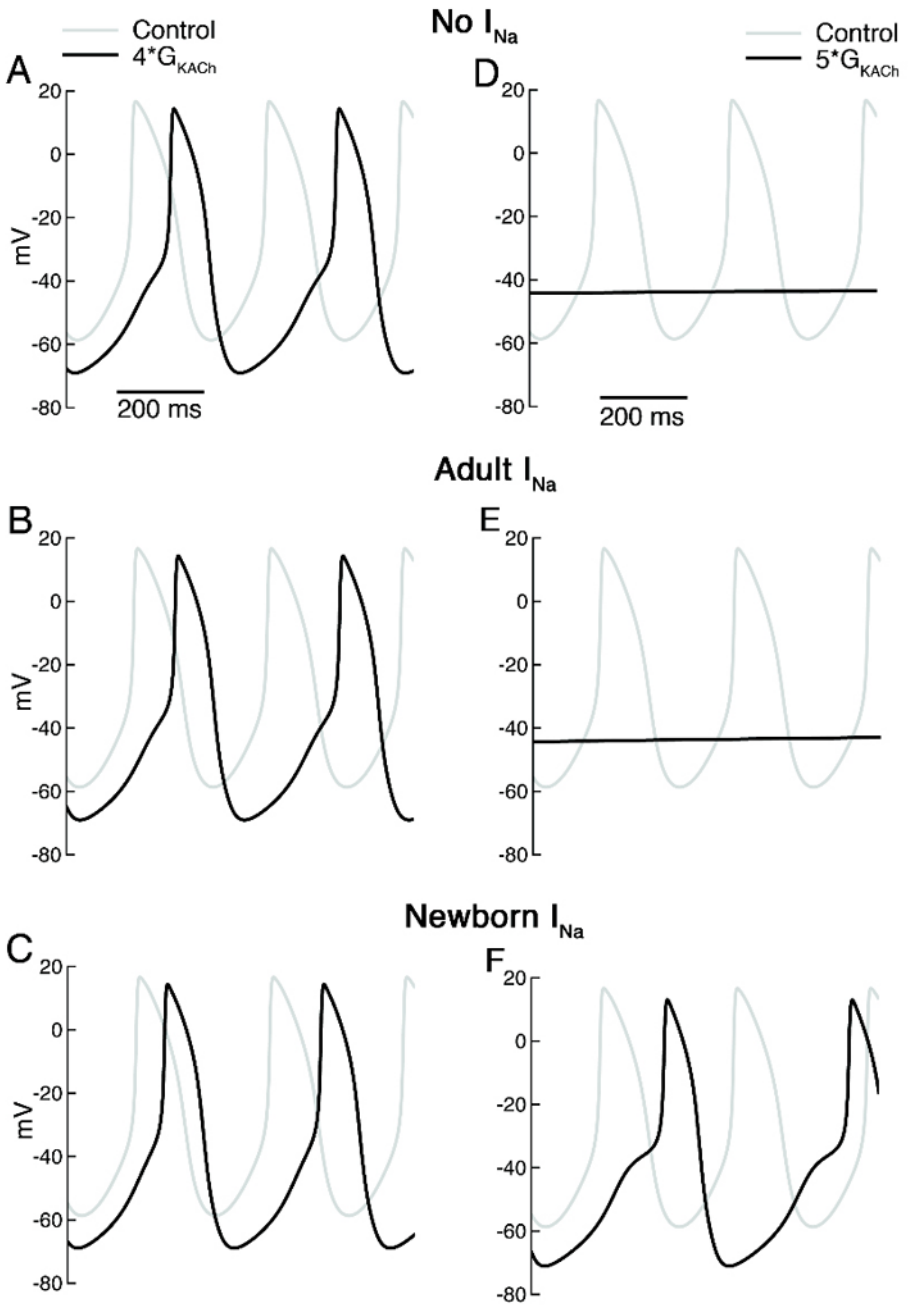

Figure 6. Simulation of vagal stimulation in presence and absence of Na current

A–C. Spontaneous APs under control conditions (gray) and with 4x background K conductance (black) without any added Na current (top), with Na current equivalent to that in adult SAN cells (middle) and with Na current of newborn SAN cells (bottom). Control cycle length (CL) was 307 ms with or without Na current addition. With 4x K conductance, CL increased to 380 and 379 ms with no I_{Na} or AD I_{Na} but to only 360 ms with NB I_{Na}. **D–F.** Spontaneous APs under control conditions (gray) and with 5x background K conductance (black) with the same 3 levels of Na current. With the higher K conductance, spontaneous activity ceased except in the case of NB I_{Na}, where CL=422 ms.

NIH-PA Author Manuscript

NIH-PA Author Manuscript

NIH-PA Author Manuscript

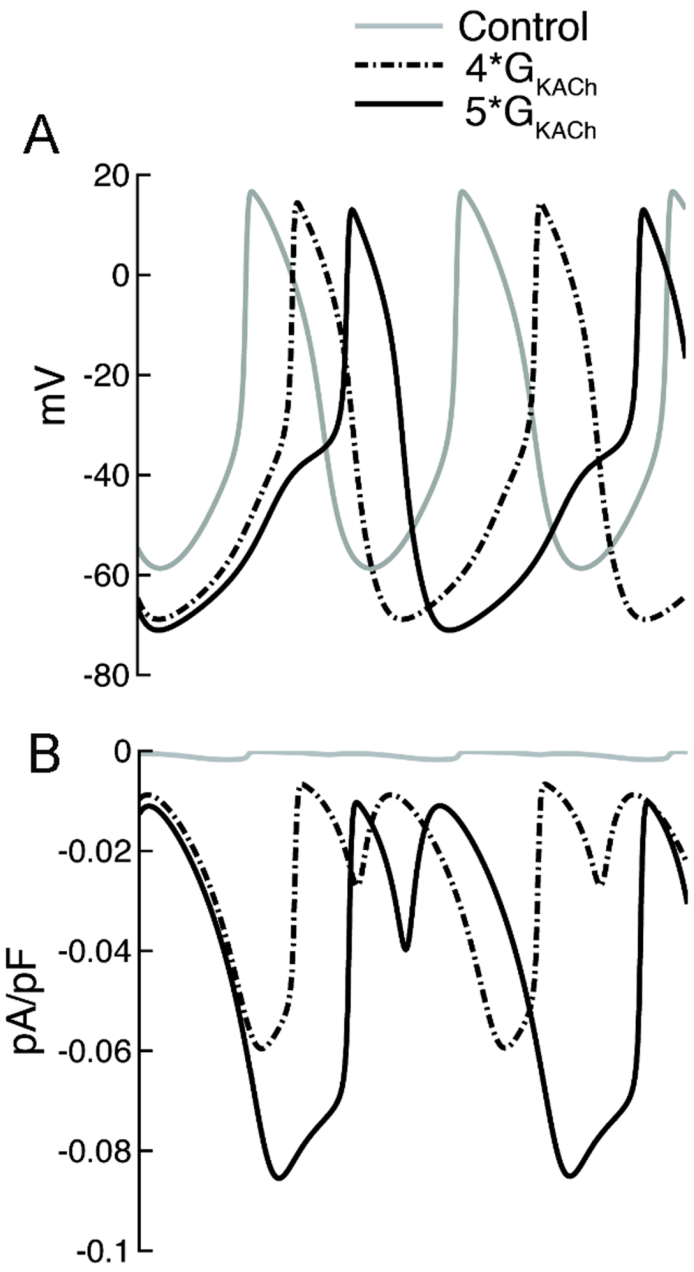

Figure 7. Effect of membrane hyperpolarization on I_{Na} in the newborn model

A. Simulated spontaneous action potentials under control conditions (gray) and with 4x (broken black) and 5x (solid black) background K conductance. **B.** Calculated Na current flowing during spontaneous activity depicted in panel A. There is an absence of significant current flow during control conditions. When background K conductance is increased, Na current flows during both diastole and the AP upstroke.

NIH-PA Author Manuscript
NIH-PA Author Manuscript
NIH-PA Author Manuscript

TABLE I

Current Parameters in Canine SAN Cells of Different Ages

		NEWBORN	YOUNG	ADULT
Capacitance		17.2±0.9	19.6±1.1	50.8±3.1*,**
		(n=11)	(n=17)	(n=44)
I_f	Density	17.2±6.2	8±2.9	9.6±1
	(pA/pF)	(n=3)	(n=3)	(n=4)
	Midpoint	82.9±5.2	90.3±2.9	84.5±2.1
	(mV)	(n=3)	(n=3)	(n=4)
I_{Na}	Occurrence	81.8	94.1	93.2
	(% of cells)	(n=11)	(n=17)	(n=44)
	Peak density	68.5±16	15.2±2.5*	9.0±2.1*,**
	(pA/pF)	(n=5; from −90)	(n=6)	(n=7)
	Activation Midpoint	−38±2.2	−35±2.2	−37.5±2.3
	(mV)	(n=5)	(n=6)	(n=7)
	Activation Slope	6.7±0.6	6.6±0.6	7.8±0.9
	(mV)	(n=5)	(n=6)	(n=7)
	Inactivation Midpoint	−89.7±0.7	−95.1±1.2*	−93.4±1.9
	(mV)	(n=3)	(n=5)	(n=9)
	Inactivation Slope	6±0.5	6.5±0.4	6.2±0.3
	(mV)	(n=3)	(n=5)	(n=9)
	TTX inhibition	46.7±6.9	59.9±4.1	90.7±3.3*,**
	(%;100 nmol/L)	(n=7)	(n=11)	(n=19)

* significantly different ($p<0.05$) from newborn

** significantly different from young